Synthesis and Structures of the μ-Vinylidene Binuclear Nickel Complexes $[Ni_2(\mu\text{-}CCH_2)(dmpm)_2Cl_2]$ and $[Ni_2(\mu\text{-}CCH_2)(dppm)_2Br_2]$: Comparison of the Electronic Structures of Nickel A-Frames

Jerald D. Heise, John J. Nash, Phillip E. Fanwick,† and Clifford P. Kubiak*

Department of Chemistry, Purdue University, West Lafayette, Indiana 47907

Received July 5, 1995⊗

The reaction of bis(cyclooctadiene)nickel(0) with bis(dimethylphosphino)methane (dmpm) and 1,1-dichlorovinylidene in THF yields the vinylidene-bridged binuclear nickel A-frame complex $[Ni_2(\mu\text{-}C{=}CH_2)(dmpm)_2Cl_2]$ (**1a**). The structure of **1a** was determined by X-ray crystallography. The Ni−Ni separation is 2.898(2) Å, and the vinylidene carbon−carbon bond distance is 1.35(2) Å. The structure of the bis(diphenylphosphino)methane (dppm) bridged μ-vinylidene complex $[Ni_2(\mu\text{-}C{=}CH_2)(dppm)_2Br_2]$ (**2b**) was also determined by X-ray crystallography. The Ni−Ni separation of 2.874(2) Å for **2b** is comparable to that of **1a**. The series of μ-vinylidene nickel A-frames with substituted terminal ligands $[Ni_2(\mu\text{-}C{=}CH_2)(PR_2CH_2PR_2)_2X_2]$ (X = Cl, Br, I, R = Me; X = Cl, Br, I, NCS, OCN; R = Ph) were prepared and characterized. The nickel A-frames with different bridging ligands $[Ni_2(\mu\text{-}C{=}E)(dppm)_2Cl_2]$ (E = O, NPh) were also examined. Extended Hückel molecular orbital (EHMO) calculations indicate that the HOMO in these nickel A-frame complexes is primarily metal based and that the LUMO is derived primarily from the π^* system of the μ-C=CH$_2$ ligand. The σ-donating ability of the diphosphine ligands affects the electronic structure of these complexes primarily by stabilizing interactions between the filled d-orbital manifold and the b_2 orbital of the vinylidene fragment.

Introduction

In the last decade there has been considerable interest in the synthesis and reactivity of μ-vinylidene complexes.[1−9] We report the synthesis of a series of μ-vinylidene nickel A-frame complexes, $[Ni_2(\mu\text{-}C{=}CH_2)(dmpm)_2X_2]$ (X = Cl, Br, I) (**1a**−**c**), and the structure of $[Ni_2(\mu\text{-}C{=}CH_2)(dmpm)_2Cl_2]$ (**1a**) (dmpm = bis(dimethylphosphino)methane). The dmpm ligand is generally regarded, and often observed, to impart increased reactivity to metal complexes compared to similar complexes of the dppm ligand (dppm = bis(diphenylphosphino)methane).[10−15] Both steric and electronic factors are expected to contribute to these differences. However, few systematic studies comparing the properties of dmpm and dppm complexes with otherwise identical ligand sets have been described.

The preparation of the dmpm-bridged nickel A-frames is based on the oxidative addition approach for A-frame synthesis.[16,17] These reactions proceed through a direct addition of the diphosphine to bis(cyclooctadiene)nickel(0), followed by addition of vinylidene dichloride and halide or pseudohalide metathesis (eq 1). The utility

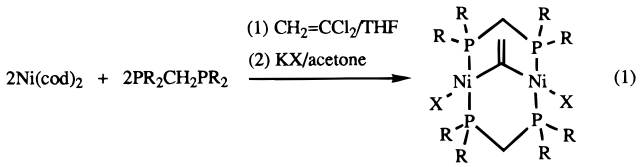

(1)

1a (R = Me, X = Cl) **2a** (R = Ph, X = Cl)
1b (R = Me, X = Br) **2b** (R = Ph, X = Br)
1c (R = Me, X = I) **2c** (R = Ph, X = I)
2d (R = Ph, X = NCS)
2e (R = Ph, X = NCO)

of this synthetic approach had been established for the preparation of the closely related dppm-bridged vinylidene A-frames, reported by Shaw, $[Ni_2(\mu\text{-}C{=}CH_2)(dppm)_2X_2]$ (X = Cl, Br, I, NCS) (**2a**−**d**),[4] as well as for the complexes $[Ni_2(\mu\text{-}SO)(dppm)_2Cl_2]$,[17] $[Ni_2(\mu\text{-}CO)(dppm)_2Cl_2]$,[18] and $[Ni_2(\mu\text{-}CNPh)(dppm)_2Cl_2]$.[19] This

† Address correspondence pertaining to crystallographic studies to this author.

⊗ Abstract published in *Advance ACS Abstracts,* February 1, 1996.

(1) Jacobsen, E. N.; Bergman, R. G. *Organometallics* **1984**, *3*, 329−31.
(2) Dawkins, G. M.; Green, M.; Jeffery, J. C.; Stone, F. G. A. *J. Chem. Soc., Chem. Commun.* **1980**, 1120−22.
(3) Carty, A. J.; Taylor, N. J.; Sappa, E.; Tiripicchio, A. *Inorg. Chem.* **1983**, *22*, 1871−6.
(4) Fontaine, X. L. R.; Higgins, S. J.; Shaw, B. L.; Thornton-Pett, M.; Yichang, W. *J. Chem. Soc., Dalton Trans.* **1987**, *109*, 1501−1507.
(5) Kolobova, N. E.; Ivanov, L. L.; Zhvanko, O. S.; Khitrova, O. M.; Batsanov, A. S.; Struchkov, Y. T. *J. Organomet. Chem.* **1984**, *262*, 39−47.
(6) Castiglioni, M.; Giordano, R.; Sappa, E. *J. Organomet. Chem.* **1983**, *258*, 217−34.
(7) Antonova, A. B.; Kovalenko, S. V.; Korniets, E. D.; Petrovskii, P. V.; Ioganson, A. A.; Deikhina, N. A. *Inorg. Chim. Acta* **1985**, *105*, 153−63.
(8) Casey, C. P.; Konings, M. S.; Marder, S. R. *Polyhedron* **1988**, *7*, 881−902.
(9) Casey, C. P.; Meszaros, M. W.; Fagan, P. J.; Bly, R. K.; Colborn, R. E. *J. Am. Chem. Soc.* **1986**, *108*, 4053−4059.
(10) Jenkins, J. A.; Cowie, M. *Organometallics* **1992**, *11*, 2774−82.
(11) Jenkins, J. A. *Organometallics* **1992**, *11*, 2767−74.
(12) Kullberg, M. L.; Kubiak, C. P. *Inorg. Chem.* **1986**, *25*, 26−30.
(13) Kullberg, M. L.; Lemke, F. R.; Powell, D. R.; Kubiak, C. P. *Inorg. Chem.* **1986**, *24*, 3589.
(14) Manojlovic-Muir, L.; Muir, K. W.; Frew, A. A.; Ling, S. S. M.; Thompson, M. A.; Puddephatt, R. J. *Organometallics* **1984**, *3*, 1637.
(15) Johnson, K. A.; Gladfelter, W. L. *Organometallics* **1989**, *8*, 2866.
(16) Balch, A. L.; Hunt, C. T.; Lee, C.-L.; Olmstead, M. M.; Farr, J. P. *J. Am. Chem. Soc.* **1981**, *103*, 3764.
(17) Gong, J. K.; Fanwick, P. E.; Kubiak, C. P. *J. Chem. Soc., Chem. Commun.* **1990**, 1190−91.

0276-7333/96/2315-1690$12.00/0

method is used in the present study to prepare a homologous series of halide- and psuedohalide-substituted nickel A-frames of dmpm (**1a**−**c**) and dppm (**2a**−**e**). The crystal and molecular structure of one of these dppm-bridged μ-vinylidene A-frame complexes, $[Ni_2(\mu\text{-}C{=}CH_2)(dppm)_2Br_2]$ (**2b**), is also reported.

Two previously reported binuclear nickel complexes, $[Ni_2(\mu\text{-}C{=}O)(dppm)_2Cl_2]$[18] and $[Ni_2(\mu\text{-}C{=}NPh)(dppm)_2Cl_2]$,[19] are also considered in this study, and their electronic properties are compared to the μ-vinylidene compounds reported here. Hoffman and Hoffmann have shown that the LUMO in formally d^9−d^9 A-frame type molecules bridged by a single π-acceptor ligand is composed primarily of the π* system of that bridging ligand.[20] In the present study, we employ extended Hückel molecular orbital (EHMO) calculations to further examine the influences of different bridgehead π-acceptor ligands, different terminal ligands *trans* to the bridgehead, and different bridging diphosphine ligands (dppm vs dmpm) on the electronic structure of these nickel A-frame complexes.

Results and Discussion

Synthesis and Characterization of (μ-Vinylidene)-nickel A-Frames. The μ-vinylidene dmpm-bridged nickel A-frames $[Ni_2(\mu\text{-}CCH_2)(dmpm)_2X_2]$ (X = Cl, Br, I; **1a**−**c**) were synthesized similarly to the dppm-bridged series, **2a**−**d**, reported earlier.[4] The bromide and iodide complexes **1b**,**1c** were prepared from **1a** by halide metathesis. The $^{31}P\{^1H\}$ chemical shifts of **1a**−**c** are surprisingly insensitive to the terminal halide ligands and vary by less than 1 ppm. There is, however, a clear trend in the UV−vis data. The chloride (**1a**), bromide (**1b**), and iodide (**1c**) show a progressive shift of their lowest energy electronic transitions to lower energy: λ_{max} = 490, 499, and 516 nm, respectively. The ^1H NMR of **1a** indicates the presence of the μ-vinylidene ligand with a phosphorus-coupled $AA'X_2X'_2$ multiplet appearing as a deceptively simple pentet at 4.86 ppm (J(PH) = 3.3 Hz). The dmpm methylene protons appear as two components of an $ABX_2X'_2$ multiplet centered at 1.79 and 1.55 ppm, with geminal coupling constant $^2J(H_AH_B)$ = 13.5 Hz and ^2J(PH) = 3.3 Hz. The inequivalent dmpm methyl groups appear at 1.48 (s) and 1.44 (s) ppm. There are differences in the ^1H NMR data for the bromide (**1b**) and the iodide (**1c**) compared to the chloride (**1a**). The first difference concerns the vinylidene signal which becomes more complex in **1b** and emerges as a true $AA'X_2X'_2$ multiplet in **1c**. The second concerns the two dmpm methyl signals which increasingly diverge for the bromide **1b** (1.58 (s) and 1.47 (s) ppm) and the iodide **1c** (1.70 (d) and 1.50 (d) ppm). This suggests that the lower field dmpm methyl resonances correspond to the methyl groups on the side of the A-frame structure, *exo* to the vinylidene ligand and *endo* to the halide ligands.

The μ-vinylidene dppm-bridged nickel A-frames $[Ni_2(\mu\text{-}C{=}CH_2)(dppm)_2X_2]$ (X = Cl, Br, I, NCS; **2a**−**d**) were prepared as reported.[4] In addition, we have prepared the cyanate derivative **2e** as a purple crystalline material by the reaction of **2a** with KOCN. The spectroscopic data for **2e** closely agree with that for the other members of the dppm-bridged series, **2a**−**d**.[4] The $^{31}P\{^1H\}$ NMR of **2e** shows a singlet at 21.9 ppm. In the ^1H NMR, the vinylidene protons are observed at 4.35 ppm as an apparent pentet with J(PH) = 3.1 Hz, and the dppm methylene protons are observed as two components of an $ABX_2X'_2$ multiplet centered at 3.09 and 2.26 ppm. The IR spectrum shows an intense band at 2218 cm^{-1} which is assigned to the ν(CN) band of the cyanate ligand.[21] We expect N-bonded connectivity between the cyanate ligand and the nickel atoms. This was the case with the structurally characterized isothiocyanate complex[4] **2d** and is typical for cyanate metal complexes, in general.[22]

Table 1. UV−Vis Electronic Spectral Data for Nickel A-Frame Complexes in THF

compound	λ_{max} (nm)	ϵ (M^{-1} cm^{-1})
$[Ni_2(\mu\text{-}C{=}CH_2)(dmpm)_2Cl_2]$ (**1a**)	490	2444
$[Ni_2(\mu\text{-}C{=}CH_2)(dmpm)_2Br_2]$ (**1b**)	499	3265
$[Ni_2(\mu\text{-}C{=}CH_2)(dmpm)_2I_2]$ (**1c**)	516	5274
$[Ni_2(\mu\text{-}C{=}CH_2)(dppm)_2Cl_2]$ (**2a**)	526	3696
$[Ni_2(\mu\text{-}C{=}CH_2)(dppm)_2Br_2]$ (**2b**)	540	2884
$[Ni_2(\mu\text{-}C{=}CH_2)(dppm)_2I_2]$ (**2c**)	563	5931
$[Ni_2(\mu\text{-}C{=}CH_2)(dppm)_2(SCN)_2]$ (**2d**)	506	13035
$[Ni_2(\mu\text{-}C{=}CH_2)(dppm)_2(OCN)_2]$ (**2e**)	506	6018
$[Ni_2(\mu\text{-}CNPh)(dppm)_2Cl_2]$ (**3**)	610	4013
$[Ni_2(\mu\text{-}CO)(dppm)_2Cl_2]$ (**4**)	694	3135

The electronic absorption spectra of **2a**−**e** have been examined as part of our investigation. Like their dmpm-bridged counterparts (**1a**−**c**), the chloride (**2a**), bromide (**2b**), and iodide (**2c**) show a progressive shift of their lowest energy electronic transitions to lower energy: λ_{max} = 526, 540, and 563 nm, respectively. The pseudohalides, SCN^- and OCN^-, induce shifts in the energy of the lowest energy electronic transitions of **2d**,**e** to higher energy, and in both cases λ_{max} is 506 nm. Table 1 contains a summary of the UV−vis electronic absorption data for **1a**−**c**, **2a**−**e**, and the other known isoelectronic dppm-bridged nickel complexes, $[Ni_2(\mu\text{-}CNPh)(dppm)_2Cl_2]$[19] and $[Ni_2(\mu\text{-}CO)(dppm)_2Cl_2]$.[18] Two principal differences are evident from a comparison of the spectroscopic data used to characterize the dmpm-bridged (**1a**−**c**) and the dppm-bridged (**2a**−**e**) μ-vinylidene A-frame complexes. First, the dmpm-bridged complexes have ^{31}P NMR chemical shifts at fields approximately 20 ppm higher than the dppm-bridged complexes. This is less than the difference in ^{31}P NMR chemical shifts for the free ligands (dppm, −22 ppm; dmpm, −54 ppm; $\Delta\delta$ = 32 ppm) and less than the differences found in other complexes where both the dppm and dmpm analogs have been characterized.[13,15,23] Second, the dmpm-bridged complexes (**1a**−**c**) show absorption maxima in their UV−vis electronic absorption spectra that are shifted to higher energy by approximately 40 nm compared to the dppm-bridged complexes (**2a**−**c**) with otherwise identical ligand arrays, Table 1. The electronic absorption spectrum of $[Ni_2(\mu\text{-}C{=}CH_2)(dmpm)_2Cl_2]$ (**1a**) and $[Ni_2(\mu\text{-}C{=}CH_2)(dppm)_2Cl_2]$ (**2a**) are compared in Figure 1. To our knowledge, the origins of the hypsochromism exhibited

(18) Manojlovic-Muir, L.; Muir, K. W.; Davis, W. M.; Mirza, H. A.; Puddephatt, R. J. *Inorg. Chem.* **1992**, *31*, 904.
(19) Hinze, S.; Gong, J. K.; Fanwick, P.; Kubiak, C. P. *J. Organomet. Chem.* **1993**, *458*, C10−C11.
(20) Hoffman, D. M.; Hoffmann, R. *Inorg. Chem.* **1981**, *20*, 3543−3555.
(21) Norbury, A. H.; Sinha, A. I. P. *J. Chem. Soc. A* **1968**, 1589.
(22) Ross, S. D. *Inorganic Infrared and Raman Spectra*; McGraw-Hill: London, 1972; pp 136−138.
(23) Hunt, C. T.; Balch, A. L. *Inorg. Chem.* **1982**, *21*, 1641.

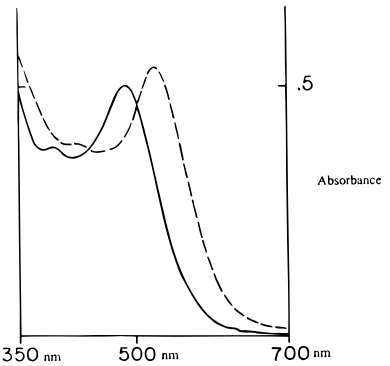

Figure 1. UV−vis spectrum of (—) $[Ni_2(\mu\text{-}C{=}CH_2)(dmpm)_2Cl_2]$, 2×10^{-4} M, and (- - -) $[Ni_2(\mu\text{-}C{=}CH_2)(dppm)_2Cl_2]$, 1×10^{-4} M, in THF.

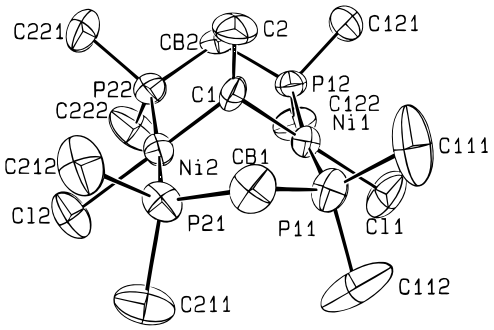

Figure 2. ORTEP drawing showing 50% probability ellipsoids of $[Ni_2(\mu\text{-}C{=}CH_2)(dmpm)_2Cl_2]$, **1a**.

by the dmpm-bridged compounds have not been discussed previously.

Crystal and Molecular Structure of $[Ni_2(\mu\text{-}C{=}CH_2)(dmpm)_2Cl_2]$ (1a). The crystal structure of **1a** consists of discrete $[Ni_2(\mu\text{-}C{=}CH_2)(dmpm)_2Cl_2]$ molecules. The molecular structure of **1a** consists of two Ni atoms bridged by two mutually *trans* dmpm ligands and the vinylidene group. The bridging vinylidene is mutually *trans* to the two terminal chloride ligands. The coordination geometry about each Ni center is thus approximately square planar, and the overall structure is typical of the A-frame geometry. This is the fourth structurally characterized nickel A-frame complex[4,17,19] and the first bridged by dmpm. An ORTEP drawing of **1a** is presented in Figure 2. Crystal data and data collection parameters for **1a** are given in Table 2. Bond distances and angles for **1a** are given in Table 3 and Table 4, respectively.

The Ni−Ni separation of 2.898(2) Å indicates the absence of a direct Ni−Ni bond. This value is similar to those found for the dppm nickel A-frames, $[Ni_2(\mu\text{-}C{=}CH_2)(dppm)_2(SCN)_2]$ (2.840(4) Å)[4] and $[Ni_2(\mu\text{-}CNPh)(dppm)_2Cl_2]$ (2.917(4) Å),[19] but significantly shorter than the separation of 3.308(1) Å found in the μ-SO complex $[Ni_2(\mu\text{-}SO)(dppm)_2Cl_2]$.[17] The bridging vinylidene carbon atom is situated nearly symmetrically between the two Ni atoms with Ni(1)−C(1) and Ni(2)−C(1) distances of 1.87(1) Å and 1.84(1) Å, respectively. The Ni(1)−C(1)−Ni(2) bond angle is 102.5(6)°, similar to the angle through the isocyanide carbon atom of $[Ni_2(\mu\text{-}CNPh)(dppm)_2Cl_2]$ (102.7(6)°).[19] The Ni−Cl bond distances of 2.243(4) and 2.241(4) Å fall within the range found in the dppm-bridged A-frames of nickel,[17−19] but the average Ni−P distance of 2.170(4) Å is significantly shorter than those found in the dppm systems. This difference is usually encountered in comparisons of dmpm- and dppm-bridged complexes.[12−14] A noteworthy structural

Table 2. Crystal Data and Data Collection Parameters for 1a and 2b

	1a	2b
formula	$Ni_2Cl_2P_4C_{12}H_{30}$	$Br_2Ni_2P_4OC_{56}H_{54}$
fw	486.59	1144.19
space group	*Cc* (No. 9)	$P2_1/n$ (No. 14)
a, Å	6.381(1)	14.653(1)
b, Å	21.631(3)	15.623(2)
c, Å,	15.926(3)	22.572(2)
β, deg	98.46(1)	95.319(6)
V, Å^3	2174(1)	5144(2)
Z	4	4
d_{calc}, g cm^{-3}	1.487	1.477
cryst dimens, mm	0.47 × 0.30 × 0.35	0.19 × 0.16 × 0.08
temp, K	293	293
radiation (wavelength)	Mo Kα (0.710 73 Å)	Cu Kα (1.541 84 Å)
monochromator	graphite	graphite
linear abs coef, cm^{-1}	22.71	42.31
abs corr applied	empirical[35]	empirical[35]
transm factors: min, max	0.31, 0.54	0.46, 0.67
diffractometer	Enraf-Nonius CAD4	Enraf-Nonius CAD4
scan method	$\omega-2\theta$	$\omega-2\theta$
h,*k*,*l* limits	−7 to 6, 0 to 23, 0 to 17	−15 to 15, 0 to 16, 0 to 24
2θ range deg	4.00−46.00	4.00−114.00
scan width, deg	0.86 + 0.35 tan θ	0.71 + 1.5 tan θ
take-off angle, deg	2.95	6.00
programs used	Enraf-Nonius Mo1EN	Enraf-Nonius Mo1EN
F_{000}	1008.0	2336.0
p-factor used in weighting	0.040	0.040
data collcd	1561	7217
unique data	1561	7217
data with $I > 3.0\sigma(I)$	1236	2882
no. of variables	179	329
largest shift/esd in final cycle	0.04	0.06
R	0.040	0.057
R_w	0.050	0.061
goodness of fit	1.377	1.170

Table 3. Selected Bond Distances (Å)[a] for 1a and 2b

compd **1a**		compd **2b**	
Ni(1)−Ni(2)	2.898(2)	Ni(1)−Ni(2)	2.874(2)
Ni(1)−Cl(1)	2.243(4)	Ni(1)−Br(1)	2.368(3)
Ni(1)−P(11)	2.167(4)	Ni(1)−P(11)	2.190(4)
Ni(1)−P(12)	2.168(4)	Ni(1)−P(12)	2.210(4)
Ni(1)−C(1)	1.87(1)	Ni(1)−C(1)	1.86(1)
Ni(2)−Cl(2)	2.241(4)	NI(2)−Br(2)	2.365(2)
Ni(2)−P(21)	2.170(4)	Ni(2)−P(21)	2.202(4)
Ni(2)−P(22)	2.176(4)	Ni(2)−P(22)	2.204(4)
Ni(2)−C(1)	1.84(1)	Ni(2)−C(1)	1.87(1)
P(11)−C(B1)	1.82(1)	P(11)−C(1B)	1.86(1)
P(11)−C(111)	1.82(2)	P(11)−C(1111)	1.83(1)
P(11)−C(112)	1.81(2)	P(11)−C(1121)	1.83(1)
P(12)−C(B2)	1.83(1)	P(12)−C(2B)	1.83(1)
P(12)−C(121)	1.80(2)	P(12)−C(1211)	1.82(1)
P(12)−C(122)	1.80(2)	P(12)−C(1221)	1.82(1)
P(21)−C(B1)	1.80(1)	P(21)−C(1B)	1.83(1)
P(21)−C(211)	1.80(2)	P(21)−C(2111)	1.79(1)
P(21)−C(212)	1.82(2)	P(21)−C(2121)	1.83(1)
P(22)−C(B2)	1.83(1)	P(22)−C(2B)	1.83(1)
P(22)−C(221)	1.81(2)	P(22)−C(2211)	1.81(1)
P(22)−C(222)	1.82(2)	P(22)−C(2221)	1.84(1)
C(1)−C(2)	1.35(2)	C(1)−C(2)	1.33(2)
		C(2)−H(21)	1.1(1)
		C(2)−H(22)	0.8(1)

[a] Numbers in parentheses are estimated standard deviations in the least significant digits.

Table 4. Selected Bond Angles (deg)[a] for 1a and 2b

compd **1a**		compd **2b**	
Ni(2)−Ni(1)−Cl(1)	141.7(2)	Ni(2)−Ni(1)−Br(1)	141.2(1)
Ni(2)−Ni(1)−P(11)	91.6(1)	Ni(2)−Ni(1)−P(11)	94.2(1)
Ni(2)−Ni(1)−P(12)	91.1(1)	Ni(2)−Ni(1)−P(12)	90.4(1)
Ni(2)−Ni(1)−C(1)	38.4(4)	Ni(2)−Ni(1)−C(1)	39.7(4)
Cl(1)−Ni(1)−P(11)	92.2(2)	Br(1)−Ni(1)−P(11)	94.6(1)
Cl(1)−Ni(1)−P(12)	92.5(2)	Br(1)−Ni(1)−P(12)	94.8(1)
Cl(1)−Ni(1)−C(1)	179.1(4)	Br(1)−Ni(1)−C(1)	177.0(4)
P(11)−Ni(1)−P(12)	168.7(2)	P(11)−Ni(1)−P(12)	158.6(2)
P(11)−Ni(1)−C(1)	86.9(4)	P(11)−Ni(1)−C(1)	82.3(4)
P(12)−Ni(1)−C(1)	88.4(4)	P(12)−Ni(1)−C(1)	88.1(4)
Ni(1)−Ni(2)−Cl(2)	141.1(1)	Ni(1)−Ni(2)−Br(2)	139.16(9)
Ni(1)−Ni(2)−P(21)	91.2(1)	Ni(1)−Ni(2)−P(21)	92.3(1)
Ni(1)−Ni(2)−P(22)	91.6(1)	Ni(1)−Ni(2)−P(22)	92.4(1)
Ni(1)−Ni(2)−C(1)	39.1(4)	Ni(1)−Ni(2)−C(1)	39.4(4)
Cl(2)−Ni(2)−P(21)	92.7(2)	Br(2)−Ni(2)−P(21)	95.6(1)
Cl(2)−Ni(2)−P(22)	92.3(2)	Br(2)−Ni(2)−P(22)	95.3(1)
Cl(2)−Ni(2)−C(1)	179.5(4)	Br(2)−Ni(2)−C(1)	177.9(4)
P(21)−Ni(2)−P(22)	168.3(2)	P(21)−Ni(2)−P(22)	157.3(2)
P(21)−Ni(2)−C(1)	86.7(4)	P(21)−Ni(2)−C(1)	83.3(4)
P(22)−Ni(2)−C(1)	88.2(4)	P(22)−Ni(2)−C(1)	86.3(4)
Ni(1)−P(11)−C(B1)	116.1(4)	Ni−(1)−P(11)−C(1B)	116.3(4)
Ni(1)−P(11)−C(111)	112.0(7)	Ni(1)−P(11)−C(1111)	105.3(4)
Ni(1)−P(11)−C(112)	115.4(7)	Ni(1)−P(11)−C(1121)	122.6(4)
C(B1)−P(11)−C(111)	104.1(9)	C(1B)−P(11)−C(1111)	105.3(6)
C(B1)−P(11)−C(112)	104.3(8)	C(1B)−P(11)−C(1121)	101.6(6)
C(111)−P(11)−C(112)	104(1)	C(1111)−P(11)−C(1211)	104.1(6)
Ni(1)−P(12)−C(B2)	116.8(4)	Ni(1)−P(12)−C(2B)	113.9(4)
Ni(1)−P(12)−C(121)	114.1(6)	Ni(1)−P(12)−C(1211)	107.5(4)
Ni(1)−P(12)−C(122)	116.1(6)	Ni(1)−P(12)−C(1221)	122.0(5)
C(B2)−P(12)−C(121)	101.9(7)	C(2B)−P(12)−C(1211)	104.2(6)
C(B2)−P(12)−C(122)	103.2(7)	C(2B)−P(12)−C(1221)	103.1(6)
C(121)−P(12)−C(122)	102.7(9)	C(1211)−P(12)−C(1221)	104.5(6)
Ni(2)−P(21)−C(B1)	116.4(5)	Ni(2)−P(21)−C(1B)	117.3(4)
Ni(2)−P(21)−C(211)	116.0(5)	Ni(2)−P(21)−C(2111)	109.2(4)
Ni(2)−P(21)−C(212)	111.6(5)	Ni(2)−P(21)−C(2121)	121.6(4)
C(B1)−P(21)−C(211)	105.2(8)	C(1B)−P(21)−C(2111)	101.3(6)
C(B1)−P(21)−C(212)	103.3(7)	C(1B)−P(21)−C(2121)	103.3(6)
C(211)−P(21)−C(212)	102.7(8)	C(2111)−P(21)−C(2121)	101.2(6)
Ni(2)−P(22)−C(B2)	116.5(4)	Ni(2)−P(22)−C(2B)	114.4(4)
Ni(2)−P(22)−C(221)	110.8(7)	Ni(2)−P(22)−C(2211)	108.5(4)
Ni(2)−P(22)−C(222)	116.8(6)	Ni(2)−P(22)−C(2221)	122.8(4)
C(B2)−P(22)−C(221)	103.8(8)	C(2B)−P(22)−C(2211)	104.6(6)
C(B2)−P(22)−C(222)	103.9(8)	C(2B)−P(22)−C(2221)	101.3(6)
C(221)−P(22)−C(222)	103(1)	C(2211)−P(22)−C(2221)	103.3(6)
Ni(1)−C(1)−Ni(2)	102.5(6)	Ni(1)−C(1)−Ni(2)	101.0(6)
Ni(1)−C(1)−C(2)	127.1(9)	Ni(1)−C(1)−C(2)	131(1)
Ni(2)−C(1)−C(2)	130.4(9)	Ni(2)−C(1)−C(2)	128(1)
P(11)−C(B1)−P(21)	112.1(7)	C(1)−C(2)−H(21)	125(6)
P(12)−C(B2)−P(22)	110.1(7)	C(1)−C(2)−H(22)	115(9)
		H(21)−C(2)−H(22)	120(10)
		P(11)−C(1B)−P(21)	115.8(6)
		P(12)−C(2B)−P(22)	109.8(7)

[a] Numbers in parentheses are estimated standard deviations in the least significant digits.

aspect of **1a** is that the eight-membered $Ni_2P_4C_2$ ring system adopts a "boat" structure with the two dmpm methylene groups folded toward the *μ*-vinylidene group. This feature appears to be quite common for this class of nickel complexes,[4,17,19] structurally characterized to date, but is unusual for A-frames with similar ligands and electronic configurations in general.[24]

Crystal and Molecular Structure of [Ni_2(*μ*-C=CH_2)(dppm)$_2Br_2$] (2b). We also report the crystal and molecular structure of the dppm-bridged *μ*-vinylidene A-frame complex of nickel, **2b**.[4] The crystal structure of **2b** consists of discrete [Ni_2(*μ*-C=CH_2)(dppm)$_2$-Br_2] molecules. There are no crystallographically imposed elements of symmetry in the molecular structure. An ORTEP drawing of **2b** is presented in Figure 3. Crystal data and data collection parameters for **2b** are given in Table 2. Bond distances and angles for **2b** are

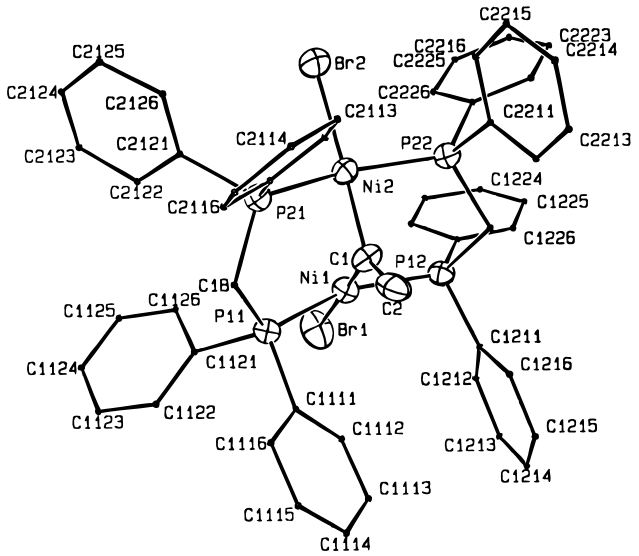

Figure 3. ORTEP drawing of [Ni_2(*μ*-C=CH_2)(dppm)$_2Br_2$], **2b**, with 50% probability ellipsoids shown on the core atoms. Fixed isotropic parameters (B = 1.0 Å^2) are shown on dppm phenyl and methylene carbon atoms for clarity.

given in Table 3 and Table 4, respectively. The Ni−Ni separation is 2.874(2) Å, similar to those found for **1a** and the other dppm nickel A-frames. The bridging vinylidene carbon atom is nearly symmetric with Ni(1)−C(1) and Ni(2)−C(1) distances of 1.86(1) and 1.87(1) Å, respectively. The eight-membered $Ni_2P_4C_2$ ring system is again in a "boat" configuration with the two dppm methylene groups folded toward the *μ*-vinylidene group. Overall, the considerable structural similarities in **1a** and **2b** are not expected. Comparison of these structures reveals fewer significant differences than are found in dmpm- and dppm-bridged palladium A-frames.[12] The palladium A-frames bridged by dmpm generally show shorter Pd−P bond distances, but these are compensated by longer Pd−X (X = Cl, Br) bond lengths when compared to the dppm-bridged complexes.[12] A similar compensation is found in the Pt−P and Pt−CH_3 bond lengths of [Pt_2(dmpm)$_2$(CH_3)$_4$] and [Pt_2(dppm)$_2$(CH_3)$_4$].[14]

Electronic Structure of (*μ*-Vinylidene)nickel A-Frames. The availability of a homologous series of dppm- and dmpm-bridged *μ*-vinyldiene A-frames naturally raises the question: what electronic structural effects dictate the similarities and differences observed in the physical properties of these compounds? Hoffman and Hoffmann have examined the electronic structure of the *μ*-CO A-frame species [Rh_2(*μ*-CO)($PH_2CH_2PH_2$)$_2$-(CO)$_2$]$^{2-}$.[20] Their results indicate that the LUMO is derived mostly from the *π** system of the *μ*-CO ligand and the HOMO is primarily metal based. Thus for A-frames with *π*-unsaturated bridgehead ligands, it appears that the LUMO will be determined by the nature of the bridgehead ligand and the HOMO will not. Extended Hückel molecular orbital calculations were undertaken for nickel A-frame systems in order to understand the important interactions relevant to their electronic structures. The interaction diagram for a [Ni_2($PH_2CH_2PH_2$)$_2$(Cl)$_2$]$^{2+}$ framework combined with the vinylidene fragment, (CH_2=C)$^{2-}$, is presented in Figure 4. The bonding between the (CH_2=C)$^{2-}$ fragment and the [Ni_2($PH_2CH_2PH_2$)$_2$(Cl)$_2$]$^{2+}$ framework results from an interaction of the b_2 and a_1 MO's with the $3b_2$ and

(24) Reinking, M. K.; Fanwick, P. E.; Kubiak, C. P. *Angew. Chem., Int. Ed. Engl.* **1989**, *28*, 1377.

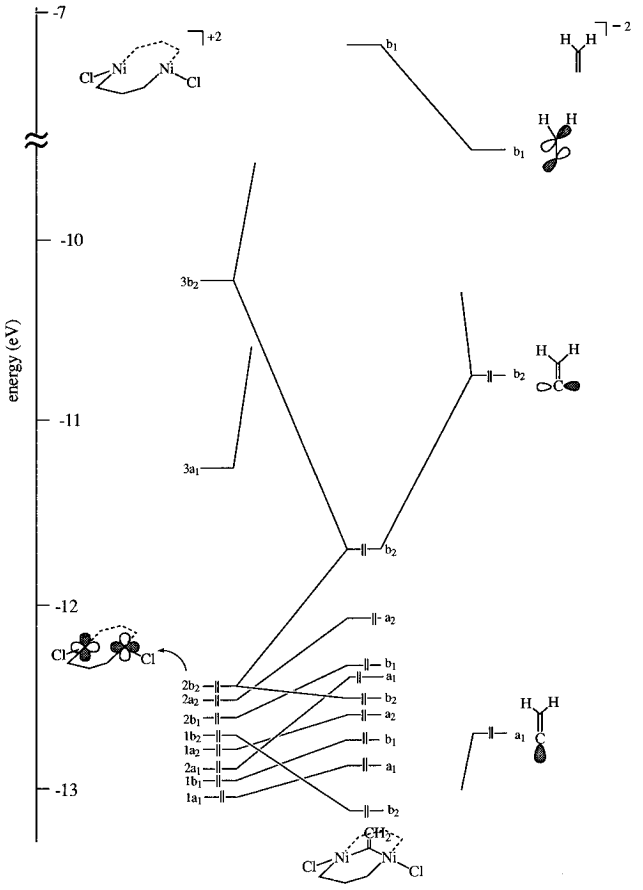

Figure 4. Extended Hückel molecular orbital energy diagram for the interaction of a $[\mu\text{-}C{=}CH_2]^{2-}$ fragment with a $[Ni_2(PH_2CH_2PH_2)_2Cl_2]^{2+}$ framework.

the $3a_1$ MO's, respectively. The HOMO has significant $d\sigma^*$ character and b_2 symmetry. The HOMO also contains a small contribution from a vinylidene p-orbital, resulting in a π-bonding interaction between the nickel centers and the vinyldene bridgehead carbon atom. An antibonding interaction exists between the vinylidene p-orbital and metal-based orbital; see Figure 5. Although the HOMO contains a metal−ligand bonding interaction, the antibonding interaction will cause this orbital to increase in energy. The HOMO is depicted in Figure 5. The LUMO has significant vinylidene π^* character and b_1 symmetry. The LUMO also contains a small contribution from a $d\pi$ pair of nickel orbitals, resulting in a π-antibonding interaction between the nickel centers and the vinylidene ligand. The LUMO is depicted in Figure 6. These results are analogous to Hoffman and Hoffmann's description of $[Rh_2(\mu\text{-}CO)(PH_2CH_2PH_2)_2(CO)_2]^{2-}$.[20]

The simplified primarily metal based HOMO and vinylidene π^* LUMO description of the nickel A-frames accommodates most of the trends in the spectroscopic properties of these compounds. First, we consider changing the bridging π-acceptor ligand. This should directly affect the energy of the LUMO. Stronger π-acceptor ligands with their lower π^* energies will result in decreased HOMO/LUMO separations. The complexes $[Ni_2(\mu\text{-}CO)(dppm)_2Cl_2]$[18] and $[Ni_2(\mu\text{-}CNPh)(dppm)_2Cl_2]$[19] have been prepared and characterized by UV−vis spectroscopy. The electronic spectra of these compounds are characterized by low-energy transitions at λ_{max} = 694 nm (μ-CO) and 610 nm (μ-CNPh),

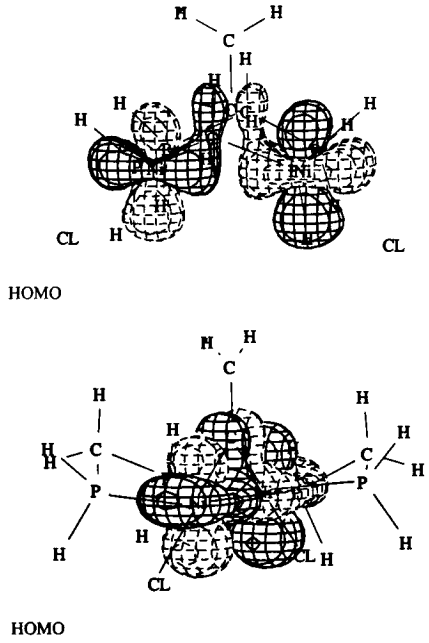

Figure 5. Extended Hückel molecular orbital plot of the HOMO resulting the interaction of a $[\mu\text{-}C{=}CH_2]^{2-}$ fragment with a $[Ni_2(PH_2CH_2PH_2)_2Cl_2]^{2+}$ framework. Top: View of $[Ni_2(PH_2CH_2PH_2)_2(C{=}CH_2)Cl_2]$. The $Ni_2(C{=}CH_2)Cl_2$ moiety is in the plane of the paper. Bottom: View of $[Ni_2(PH_2CH_2PH_2)_2(C{=}CH_2)Cl_2]$ looking down the nickel−nickel axis.

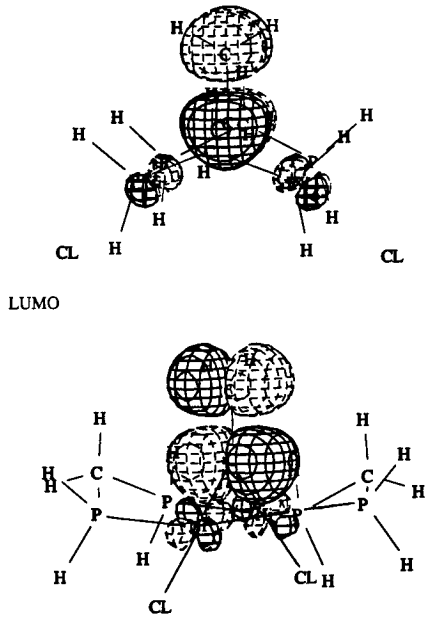

Figure 6. Extended Hückel molecular orbital plot of the LUMO resulting from the interaction of a $[\mu\text{-}C{=}CH_2]^{2-}$ fragment with a $[Ni_2(PH_2CH_2PH_2)_2Cl_2]^{2+}$ framework. Top: View of $[Ni_2(PH_2CH_2PH_2)_2(C{=}CH_2)Cl_2]$. The $Ni_2(C{=}CH_2)Cl_2$ moiety is in the plane of the paper. Bottom: View of $[Ni_2(PH_2CH_2PH_2)_2(C{=}CH_2)Cl_2]$ looking down the nickel−nickel axis.

compared to 526 nm for the μ-C=CH$_2$ A-frame (**2a**), Table 1. These results agree with the lower π^* energies of CO and CNPh compared to C=CH$_2$. It is important to note that in the solid state the complex $[Ni_2(\mu\text{-}CO)(dppm)_2Cl_2]$ does not adopt an A-frame type structure, but it has been suggested that the complex possesses an average A-frame structure in solution.[18]

Nonetheless, the spectroscopic data for $[Ni_2(\mu\text{-CO})(dppm)_2Cl_2]$ should be regarded with caution when compared to that for the other *bona fide* A-frame compounds considered in this study. With this caveat concerning the experimental data, there is still a reasonable basis to conclude that stronger π-acceptor ligands in the bridgehead position result in lower HOMO/LUMO separations.

We consider next the effects of changing the terminal halide or pseudohalide ligands. Both the dmpm-bridged (**1a**−**c**) and dppm-bridged (**2a**−**c**) A-frames show electronic transitions that in energy follow the order Cl > Br > I, Table 1. Although this is the normal ordering for the empirical "spectrochemical series" of increased d-orbital splittings by halide ligands, it is useful to consider the effect within the context of our EHMO calculations. Again, a primarily metal-based HOMO and vinylidene π*-based LUMO is important in this trend. The dσ and dπ interactions between the nickel atoms and the halogen ligands lead to metal-based $[Ni_2(PH_2CH_2PH_2)_2(X)_2]^{2+}$ fragment orbitals that in energy follow the order Cl < Br < I. This translates directly to the decreasing order of the primarily metal-based HOMO's (Cl < Br < I) and to increasing HOMO/LUMO separations (Cl > Br > I) for the series.

We consider finally the effects of different bridging diphosphine ligands. The dmpm-bridged complexes (**1a**−**c**) show absorption maxima in their UV−vis electronic absorption spectra which are shifted to higher energy by approximately 40 nm compared to the related dppm-bridged complexes (**2a**−**c**), Table 1. A direct comparison of the electronic absorption spectrum of $[Ni_2(\mu\text{-C}{=}CH_2)(dmpm)_2Cl_2]$ (**1a**) and $[Ni_2(\mu\text{-C}{=}CH_2)(dppm)_2Cl_2]$ (**2a**) is also made in Figure 1. For the purposes of these calculations, $PH_2CH_2PH_2$ (dHpm) was used to model the bridging diphosphine ligands. Structural parameters were obtained from the crystal structure of **1a** where hydrogens were substituted for methyl groups. Classically, the π-accepting ability of phosphines was believed to be solely an interaction between the phosphorus 3dπ orbitals and metal d-orbitals.[25] In recent years it has been shown that the π-accepting ability of phosphine ligands is affected by the mixing of the phosphorus 3dπ orbitals and the P−R σ* orbitals.[26−29] We find that the π-accepting ability of the diphosphines in our systems has only a minor influence on the overall electronic structure of these compounds. The dmpm ligand is a stronger σ-donor than dppm. Consequently, dmpm increases the amount of electron density on the metal centers, thus raising the energy of the d-orbital manifold. This strengthens the interaction with the b_2 orbital of the vinylidene fragment and leads to a larger HOMO−LUMO gap. The result is seen as a blue shift in the UV−vis spectra of the dmpm compounds relative to their dppm counterparts. The EHMO calculations thus do provide a model for considering the generally higher energy electronic transitions of the dmpm-bridged A-frames compared to the dppm-bridged systems. Perhaps, the real lesson of the EHMO calculations is that for nickel A-frame complexes bridged by dmpm or dppm, significant differences in ground-state electronic structure are not to be expected. Certainly, in the case of the new dmpm-bridged nickel A-frames (**1a**−**c**) reported here and compared to the dppm-bridged systems (**2a**−**c**),[4] the similarities in molecular and electronic structure far outweigh the differences.

(25) Cotton, F. A.; Wilkinson, G. *Advanced Inorganic Chemistry*, 4th ed.; Wiley: New York, 1980 p 87.
(26) Xiao, S.-X.; Trogler, W. C.; Ellis, D. E.; Berkovitch-Yellin, Z. *J. Am. Chem. Soc.* **1983**, *105*, 7033−7037.
(27) Marynick, D. S. *J. Am. Chem. Soc.* **1984**, *106*, 4064−4065.
(28) Braga, M. *Inorg. Chem.* **1985**, *24*, 2702−2706.
(29) Orpen, A. G.; Connelly, N. G. *J. Chem. Soc., Chem. Commun.* **1985**, 1310−1311.

Experimental Section

General Procedures. All manipulations were carried out under nitrogen using standard Schlenk line and drybox techniques. Solvents were degassed and purified by distillation under nitrogen from the appropriate drying agents. Ni(cod)$_2$ (cod = 1,5-cyclooctadiene), bis(dimethylphosphino)methane (dmpm), and bis(diphenylphosphino)methane (dppm) were purchased from Strem Chemicals or Aldrich (dppm) and used without further purification. ^{1}H NMR spectra were recorded on General Electric QE 300 or Varian XL-200 spectrometers with chemical shifts in ppm referenced to internal $SiMe_4$. $^{31}P\{^1H\}$ NMR spectra were recorded on General Electric QE 300 or a Varian XL-200 spectrometers operating at 121.4 and 80.96 MHz, respectively. $^{31}P\{^1H\}$ NMR chemical shifts were reported in ppm with respect to an external 85% H_3PO_4 reference. UV−vis electronic absorption spectra were recorded on an IBM 9420 spectrophotometer. Elemental analyses were determined by Galbraith Laboratories, Inc., Knoxville, TN.

Synthesis of $[Ni_2(\mu\text{-C}{=}CH_2)(dmpm)_2Cl_2]$ (1a). A 100 mL Schlenk flask was charged with Ni(cod)$_2$ (1.0 g, 3.64 mmol), 20 mL of THF, and a stir bar. In a separate flask, dmpm (0.57 mL, 3.64 mmol) was dissolved in 10 mL of THF. The dmpm solution was transferred by cannula into the Schlenk flask with continuous stirring. To the resulting red solution was added 1,1-dichlorovinylidene (0.15 mL, 1.82 mmol) by syringe. The solution was stirred vigorously for 5 min after which time 30 mL of hexane was added. The reaction flask was then placed in a freezer at −20 °C overnight and then filtered to produce a brick red microcrystalline solid and a dark red solution. The solid was placed on a fine frit, and a minimum amount of THF was used to extract the soluble portion through the frit, leaving a small quantity of an insoluble black solid presumed to be nickel metal. The extract was placed in a small round bottom flask. Clusters of needlelike crystals were obtained by layering an equal volume of hexane over the filtrate solution and storing in a freezer (yield: 0.43 g, 48% based on Ni). Anal. Calcd for $Ni_2C_{12}H_{30}P_4Cl_2$: C, 29.62; H, 6.21; P, 25.46. Found: C, 29.50; H, 6.66; P, 25.18. $^{31}P\{^1H\}$ NMR (CD_2Cl_2): δ −0.1 (s). ^{1}H NMR (CD_2Cl_2): δ 4.86 (p, C=CH_2, J(PH) = 3.30 Hz), 1.79, 1.55 (m, PCH_AH_BP), 1.48, 1.44 (s, PMe_AMe_B). UV−vis data appear in Table 1.

Synthesis of $[Ni_2(\mu\text{-C}{=}CH_2)(dmpm)_2Br_2]$ (1b). **1a** (0.20 g, 0.41 mmol) was added to a 50 mL acetone solution of KBr (0.49 g, 4.1 mmol). The mixture was stirred for 5 min. The acetone was removed under vacuum, and the remaining solid was extracted with CH_2Cl_2 and recrystallized from CH_2Cl_2/hexane. This resulted in the formation of a red microcrystalline solid (yield: 0.17 g, 71% based on **1a**). Anal. Calcd for $Ni_2C_{12}H_{30}P_4Br_2$: C, 25.05; H, 5.25; Br, 27.77. Found: C, 25.19; H, 5.45; Br, 27.44. $^{31}P\{^1H\}$ NMR (CD_2Cl_2): δ −0.2 (s). ^{1}H NMR (CD_2Cl_2): δ 4.89 (p, C=CH_2, J(PH) = 1.2 Hz), 1.85, 1.14 (m, PCH_AH_BP), 1.58, 1.47 (s, PMe_AMe_B). UV−vis data appear in Table 1.

Synthesis of $[Ni_2(\mu\text{-C}{=}CH_2)(dmpm)_2I_2]$ (1c). **1a** (0.20 g, 0.41 mmol) was added to a 50 mL acetone solution of KI (0.68 g, 4.1 mmol). The mixture was stirred for 5 min. The acetone was removed under vacuum, and the remaining solid was extracted with CH_2Cl_2 and recrystallized from CH_2Cl_2/hexane. This resulted in the formation of a dark purple microcrystalline solid (yield: 0.21 g, 78% based on **1a**). Anal. Calcd for $Ni_2C_{12}H_{30}P_4I_2$: C, 21.53; H, 4.52. Found: C, 21.71; H, 4.77.

$^{31}P\{^1H\}$ NMR (CD_2Cl_2): δ 0.4 (s). ^1H NMR (CD_2Cl_2): δ 4.88 (m, C=CH_2), 1.94, 1.20 (m, PCH_AH_BP), 1.70, 1.50 (d, PMe_AMe_B, $J(PH_A) = 5.2$ Hz, $J(PH_B) = 5.3$ Hz). UV−vis data appear in Table 1.

Synthesis of [$Ni_2(\mu$-C=$CH_2)(dppm)_2X_2$] (X = Cl, Br, I, SCN) (2a−d). These compounds were prepared as described previously by Shaw et al.[4] UV−vis data appear in Table 1.

Synthesis of [$Ni_2(\mu$-C=$CH_2)(dppm)_2(OCN)_2$] (2e). This complex was prepared by a modification of the procedure reported by Shaw et. al.[4] **2a** (0.20 g, 0.20 mmol) was added to a 25 mL acetone solution of KOCN (0.16 g, 2.0 mmol). The mixture was stirred for 5 min. The solvent was removed under vacuum, and the solid was extracted with CH_2Cl_2. Recrystallization from CH_2Cl_2/hexane gave a purple crystalline solid (yield: 0.15 g, 75% based on **1a**). Anal. Calcd for $Ni_2C_{54}H_{46}P_4O_2N_2$: C, 65.10; H, 4.65. Found: C, 64.51; H, 4.87. $^{31}P\{^1H\}$ NMR (CD_2Cl_2): δ 21.9 (s). ^1H NMR (CD_2Cl_2): δ 4.35 (p, C=CH_2), 3.09, 2.26 (m, PCH_AH_BP), 7.65−7.22 (m, C_6H_5).

X-ray Structure Determination of [$Ni_2(\mu$-C=$CH_2)$-$(dmpm)_2Cl_2$] (1a). X-ray-quality crystals were grown from a THF/hexane solution as orange needles. Data were collected on an Enraf-Nonius CAD4 diffractometer, and the structure was solved using the MULTAN11/82 program package. The crystallographic data and collection parameters are summarized in Table 2. Selected bond distances and bond angles are given in Tables 3 and 4, respectively.

X-ray Structure Determination of [$Ni_2(\mu$-C=$CH_2)$-$(dmpm)_2Br_2$] (2b). X-ray-quality crystals were grown in a THF/hexane solution as red-orange plates. Data were collected on an Enraf-Nonius CAD4 diffractometer, and the structure was solved with the SHELX-86 program package. The crystallographic data and collection parameters are summarized in Table 2. Selected bond distances and bond angles are given in Tables 3 and 4, respectively.

Extended Hückel Molecular Orbital Calculations. All calculations were performed by using the extended Hückel method,[30,31] with weighted H_{ij}'s[32] and using the FORTICON8 program.[33] The geometry for the complex, and the fragments used to construct the interaction diagram, were based on the crystal structure of **1a**. In the case of $PH_2CH_2PH_2$, a P−H bond length of 1.44 Å was assumed. The parameters used in our calculations for C, H, P, and Cl are the standard ones.[30,31] The previously reported parameters for Ni were used without modification.[34]

Acknowledgment is made to the NSF (Grant CHE-9319173) for support of this work. We are also grateful to the NSF for support of the Chemical X-ray Diffraction Facility at Purdue. We are particularly grateful to Professors Bruce Bursten and George Stanley for their careful and insightful suggestions regarding this work.

Supporting Information Available: Text describing X-ray procedures and tables consisting of crystal data and data collection parameters, positional and thermal parameters for all atoms, temperature factor expressions, bond distances, bond angles, and torsional angles for **1a** and **2b** (41 pages). Ordering information is given on any current masthead page.

OM9505165

(30) Hoffmann, R.; Lipscomb, W. N. *J. Chem. Phys.* **1962**, *36*, 2179 and 2872.
(31) Hoffmann, R. *J. Chem. Phys.* **1963**, *39*, 1397.
(32) Ammeter, J. H.; Burgi, H. B.; Thibeault, J. C.; Hoffmann, R. *J. Am. Chem. Soc.* **1978**, *100*, 3686.
(33) Howell, J.; Rossi, A.; Wallace, D.; Haraki, K.; Hoffmann, R. Quantum Chemistry Program Exchange, Bloomington, IN 47405.
(34) Albright, T. A.; Hoffmann, R.; Thibeault, J. C.; Thorn, D. L. *J. Am. Chem. Soc.* **1979**, *101*, 3801.
(35) Walker, N.; Stuart, D. *Acta Crystallogr., Sect. A* **1983**, *A39*, 158.